



FP7-600716

Whole-Body Compliant Dynamical Contacts in Cognitive Humanoids

D5.4

Validation scenario 4: learning how to stand up with the help of a human caregiver.

| | |
|----------------------------|--|
| Editor(s) | Francesco Nori |
| Responsible Partner | IIT |
| Affiliations | ¹ IIT |
| Status-Version: | Draft-1.0 |
| Date: | Feb. 28, 2017 |
| EC Distribution: | Consortium |
| Project Number: | 600716 |
| Project Title: | Whole-Body Compliant Dynamical Contacts in Cognitive Humanoids |

| | |
|------------------------------------|---|
| Title of Deliverable: | Validation scenario 4: learning how to stand up with the help of a human caregiver. |
| Date of delivery to the EC: | 28/2/2016 |

| | |
|--|---|
| Workpackage responsible for the Deliverable | deliv WP5 |
| Editor(s): | Daniele Pucci |
| Contributor(s): | Daniele Pucci, Francesco Romano, Jorhabib Eljaik, Silvio Traversaro, Vincent Padois, Francesco Nori, Claudia Latella, Marta Lorenzini, Maria Lazzaroni |
| Reviewer(s): | |
| Approved by: | All Partners |
| Abstract | This deliverable discusses the technical details and choices for the implementation of the year-4 validation scenario of the CoDyCo project. The validation scenario aims at verifying the control performances in the case the humanoid robot iCub must balance while interacting with humans. Physical human-robot interaction is a field of growing interest among the scientific community. One of the main challenges is to replicate the physical mutual interaction occurring during a collaborative task between humans. For this purpose, the knowledge about human whole-body motions and forces is mandatory but the current state of the art on robots ability in estimating them is not sufficient to yield to a suitable interaction. This paper is an extended version of our previous work and a first attempt to go into this direction inasmuch as a first human-robot interaction task was investigated. The results prove that our framework is able to estimate the human dynamics variables also in a context of human-robot interaction by laying the foundation for more complex collaboration scenarios. |
| Keyword List: | Whole-body human dynamics, Human-robot physical collaboration, Probabilistic sensor fusion algorithm |

Document Revision History

| Version | Date | Description | Author |
|---------------|-------------|--|---------------|
| First draft | 19 Feb 2017 | In this version we simply write down a few considerations on the fourth year validation scenario as discussed after the mid-year CoDyCo meeting in Birmingham. | Daniele Pucci |
| Final version | 27 Feb 2016 | None | Daniele Pucci |

Table of Contents

| | | |
|----------|--|-----------|
| 1 | Introduction | 4 |
| 2 | Background | 4 |
| 2.1 | Problem statement | 5 |
| 3 | Human Body Modelling | 6 |
| 3.1 | Kinematic properties | 6 |
| 3.2 | Dynamic properties | 6 |
| 4 | Probabilistic Sensor Fusion Algorithm | 8 |
| 5 | Experimental Design | 9 |
| 5.1 | Human configuration | 9 |
| 5.2 | Robot configuration | 10 |
| 5.3 | Procedure protocol | 11 |
| 5.4 | Data processing | 12 |
| 6 | Experimental Results | 13 |
| 6.1 | Torques estimation | 13 |
| 6.2 | Robustness test | 15 |
| 6.3 | Incremental sensor fusion analysis | 16 |
| 7 | Conclusions and Future Works | 18 |

1 Introduction

The understanding of the human dynamics and the way in which its contribute can be applied to enhance a physical human-robot interaction (pHRI) are two of the most promising challenges for the scientific community due mainly to their enormous and to-be-developed potential in industrial scenarios, ergonomics context, as well as in assistive and rehabilitation fields. Classical robots are built to act *for* humans, but in order to adapt their functionality to the current technological progress, the new generation of robots will have to collaborate *with* humans. This implies that the robots will be endowed with the capability to control physical collaboration through intentional interaction with humans. To achieve this condition, robots have to know mandatorily the dynamics (contact forces, internal forces, joint torques) of the human agent who they are interacting with. However the current state of the robot knowledge in observing human whole-body dynamics yields to non-proficient and unadaptive interactions.

To overcome this drawback, it is fundamental to understand what the response of the human body is while a physical interaction is occurring. The importance in retrieving this information is exemplified in Fig. 1: once the dynamic variables are computed by exploiting a dynamics estimation algorithm, the human dynamics feedback may be provided to the robot controllers. As a consequence, the robot may adjust the strategy of interaction accordingly.

This work is the first attempt to go in this direction since a first pHRI task was inserted with respect to our previous work [12] where only an investigation on the human inverse dynamics was carried out. The paper is built on the theoretical framework described in [12] from which it inherits both the notation and formulation.

The paper is structured as follows. Section 2 introduces the state-of-the-art background which the paper is based on. Section 3 presents the modelling of the human body as an articulated multi-body system. In Section 4 the adopted Gaussian probabilistic domain for the sensor fusion methodology is briefly recalled. Section 5 outlines the experimental set-up followed by a description of the results in Section 6. Conclusions and several considerations on the pivotal role of further control and estimation developments are depicted in Section 7.

2 Background

The aim of this Section is to provide a rapid fast-forward of what is the current direction of the scientific community on this topic. Most of the studies on the pHRI take inspiration from the intrinsic behaviour of the human nature: the *mutual adaptive nature* that automatically occurs when two humans are cooperating together to accomplish a common task.

To this purpose, the importance of understanding human dynamics goes without saying and it is a crucial aspect of current state-of-the-art studies. Since humans move by minimizing jerk trajectories [7], a method based on the minimum jerk model is used as a suitable approximation for estimating the human partner motions in [13]. Here the attempt is that of incorporating human characteristics in the control strategy of the

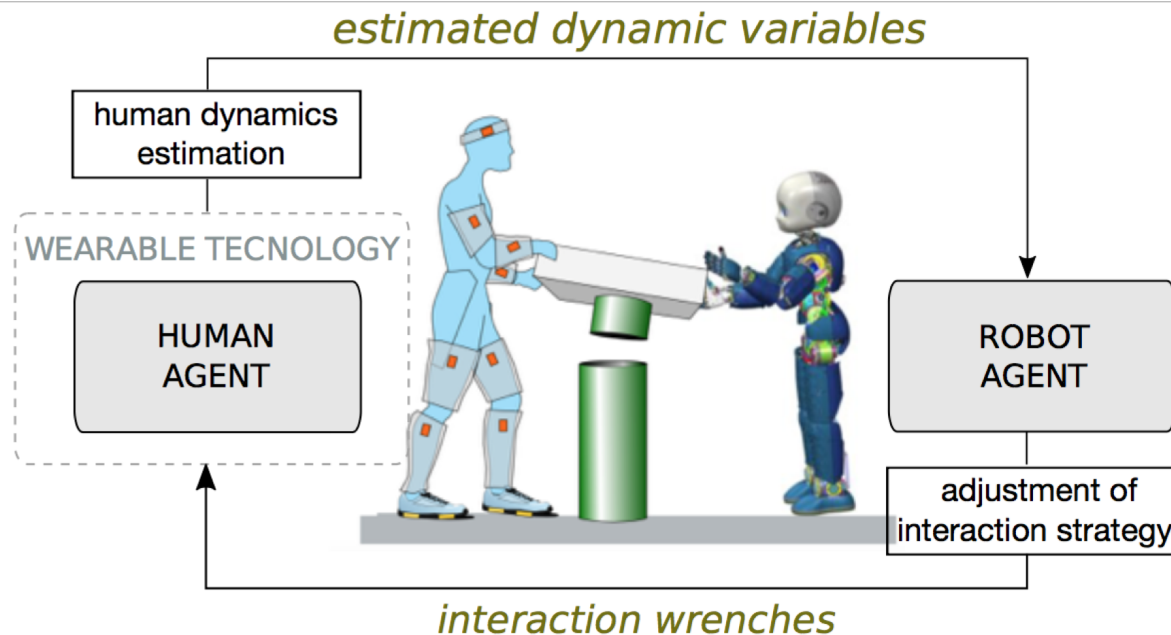


Figure 1: An example of pHRI scenario: the human agent is provided with a wearable technology and an estimation algorithm allows to retrieve information about his dynamics. By properly embedding estimations in the control loop of the robot, the intentional collaboration may be enhanced.

robot. The weakness in this type of approach, however, lies in the pre-determination of the task and in the role that the robot has to play in the task execution. Furthermore, the minimum jerk model reliability decreases considerably if the human partner decides to apply non-scheduled trajectory changes during the task [17]. Another route for pHRI is the *imitation learning* approach, where the movements of two human actors are typically retrieved with motion capture techniques, clustered in motion database ([8], [11], [23]) and then used to learn the interaction skills ([1], [21], [14]).

2.1 Problem statement

Unlike the current leaning, we want to pay more attention on the key role that a proper sensing technology for human beings together with dynamics estimation algorithms may offer for retrieving whole-body motions and interaction forces. More in detail, our work will be based on the formalism adopted for humanoid robots by making the assumption of modelling the human body as a articulated rigid multi-body system. The advantage of this choice is evident since it allows to handle both systems with the same mathematical tools. In this domain, the application of the Euler-Poincaré formalism [15] leads to three sets of equations describing: *i*) the motion of the robot, *ii*) the motion characterizing the human, *iii*) the linking equations characterizing the contacts between human and robot.

$$i) \quad \mathbf{M}(\mathbf{q})\dot{\mathbf{v}} + \mathbf{C}(\mathbf{q}, \mathbf{v})\mathbf{v} + \mathbf{G}(\mathbf{q}) = \begin{bmatrix} \mathbf{0} \\ \boldsymbol{\tau} \end{bmatrix} + \mathbf{J}^\top(\mathbf{q})\mathbf{f}$$

$$ii) \quad \mathbb{M}(\bar{\mathbf{q}})\dot{\bar{\mathbf{v}}} + \mathbb{C}(\bar{\mathbf{q}}, \bar{\mathbf{v}})\bar{\mathbf{v}} + \mathbb{G}(\bar{\mathbf{q}}) = \begin{bmatrix} \mathbf{0} \\ \boldsymbol{\tau} \end{bmatrix} + \mathbb{J}^\top(\bar{\mathbf{q}})\mathbf{f}$$

$$iii) \quad [\mathbf{J}(\mathbf{q}) \quad \mathbb{J}(\bar{\mathbf{q}})] \begin{bmatrix} \dot{\mathbf{v}} \\ \dot{\bar{\mathbf{v}}} \end{bmatrix} + [\dot{\mathbf{J}}(\mathbf{q}) \quad \dot{\mathbb{J}}(\bar{\mathbf{q}})] \begin{bmatrix} \mathbf{v} \\ \bar{\mathbf{v}} \end{bmatrix} = \mathbf{0}$$

Equations *i*) and *ii*) are floating base system representations of the dynamics of the robot and human models, respectively. Vectors \mathbf{q} and $\bar{\mathbf{q}}$ represent the configuration space (i.e. the position and orientation of a chosen frame, called base frame, and the joints configuration) of the two systems. The velocity is represented by \mathbf{v} and $\bar{\mathbf{v}}$ for robot and human systems, respectively. The matrices \mathbb{M} , \mathbb{C} , \mathbb{G} and \mathbb{M} , \mathbb{C} , \mathbb{G} denote the mass matrix, Coriolis matrix and the gravity bias term for the robot and the human systems, respectively. The forces the two systems exchange are denoted by \mathbf{f} , which owns a proper dimension depending on the number of wrenches¹ exchanged during the interaction task². The Jacobians associated with the forces \mathbf{f} are denoted by $\mathbf{J}(\mathbf{q})$ and $\mathbb{J}(\bar{\mathbf{q}})$. In *iii*) we make the assumption of rigid contacts between the two systems.

3 Human Body Modelling

We propose a human body reference model as an articulated multi-body skeleton with rigid bodies connected by 3 Degrees-of-Freedom (DoF) joints. Kinematic and dynamic properties are defined as follows.

3.1 Kinematic properties

Inspired by the biomechanical model developed for the Xsens MVN motion capture system [19] shown in Fig. 3b, our model consists of a set of 23 rigid bodies with simple geometric shapes (parallelepiped, cylinder, sphere). The origin of each link is located at the parent joint origin, (i.e., the joint that connects the link to its parent). Figure 2b shows links and joints of the model. The dimension of each link is estimated by using data coming from motion capture acquisition.

3.2 Dynamic properties

The dynamic properties, such as center of mass and inertia tensor for each link, are not embedded in the Xsens output data since they are usually computed in a post-processing phase. Since our aim is to have a real-time estimation for the human dynamic variables, the knowledge of dynamic properties during the acquisition phase is

¹As an abuse of notation, we define as wrench a quantity that is not the dual of a twist but a vector $\in \mathbb{R}^6$ containing both the forces and the related moments.

²For the sake of simplicity, we omitted the forces the two systems exchange with the external environment (i.e., the ground) from the formulation of *i*) and *ii*). As a straightforward consequence, the linking equations between each system with the external environment are not considered.

³The RGB (Red-Green-Blue) convention for *x-y-z* axes is adopted throughout the paper.

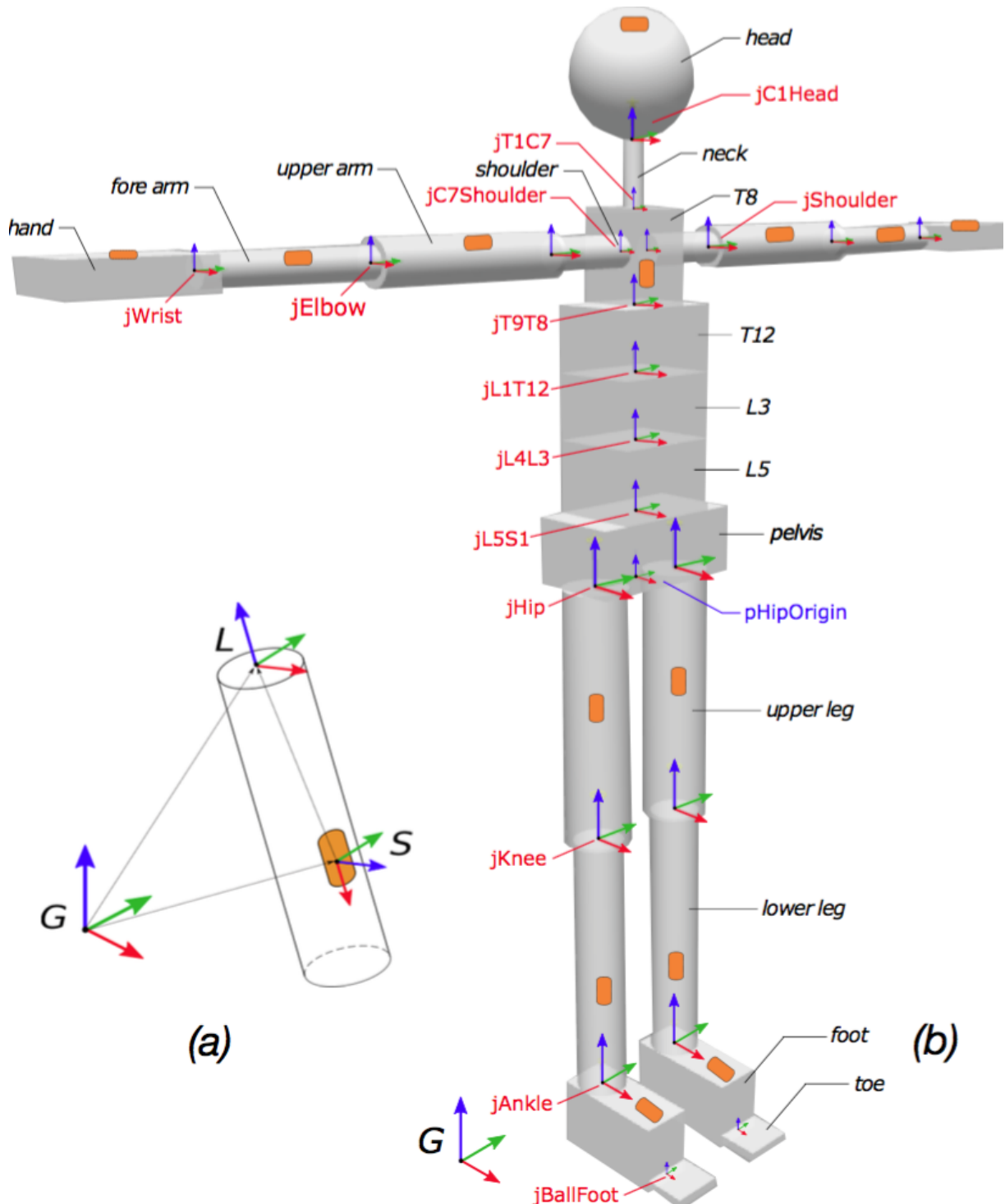


Figure 2: (a) Sensor attached to a generic link. (b) Human body reference model with labels for links and joints and with sensors distributed in the Xsens suit. Reference frames are also shown³.

mandatory [5]. Since it is impractical to retrieve these quantities in-vivo for humans, we relied on the available anthropometric data in literature ([22], [10]) starting from the total body mass of the subject, under the assumptions of geometric approximation and of homogeneous density for the rigid bodies ([9], [24]).

4 Probabilistic Sensor Fusion Algorithm

In this Section we briefly recall the probabilistic method for estimating dynamic variables of an articulated mechanical system by exploiting the so-called sensor fusion information, already presented in our previous work (the reader should refer to [12] for a more thorough presentation).

From a theoretical point of view, we describe our model as a mechanical system represented by an oriented kinematic tree with N_B moving links and n -DoFs. Note that $n = n_1 + \dots + n_{N_B}$ is the total number of DoFs of the system. The generic i -th link and its parent are coupled with a joint i following the topological Denavit-Hartenberg convention for joint numbering [4]. We are interested in computing an estimation of a vector of *dynamics variables* \mathbf{d} defined as:

$$\begin{aligned}\mathbf{d} &= [\mathbf{d}_1^\top \quad \mathbf{d}_2^\top \quad \dots \quad \mathbf{d}_{N_B}^\top]^\top \in \mathbb{R}^{24N_B+2n}, \\ \mathbf{d}_i &= [\mathbf{a}_i^\top \quad \mathbf{f}_i^B{}^\top \quad \mathbf{f}_i^\top \quad \boldsymbol{\tau}_i \quad \mathbf{f}_i^{x\top} \quad \ddot{\mathbf{q}}_i]^\top \in \mathbb{R}^{24+2n_i},\end{aligned}$$

where \mathbf{a}_i is the i -th body spatial acceleration, \mathbf{f}_i^B is the net wrench, \mathbf{f}_i is the internal wrench exchanged from the parent link to the i -th link, $\boldsymbol{\tau}_i \in \mathbb{R}^{n_i}$ is the torque at the joint, \mathbf{f}_i^x is the external wrench applied by the environment to the link and $\ddot{\mathbf{q}}_i \in \mathbb{R}^{n_i}$ is the joint acceleration. The system can interact with the surrounding environment, and the result of this interaction is reflected in the presence of the external wrenches \mathbf{f}_i^x .

The dynamics of the mechanical system⁴ can be obtained from the application of the Newton-Euler equations⁵ [6]. It is possible to rearrange these equations into a matrix form thus obtaining the following linear system of equations in the variable \mathbf{d} :

$$\mathbf{D}(\mathbf{q}, \dot{\mathbf{q}})\mathbf{d} + \mathbf{b}_D(\mathbf{q}, \dot{\mathbf{q}}) = \mathbf{0}, \quad (2)$$

where the matrix $\mathbf{D} \in \mathbb{R}^{(18N_B+n) \times d}$ and the bias vector $\mathbf{b}_D \in \mathbb{R}^{18N_B+n}$. We now consider the presence of N_S measurements of dynamic quantities coming from different sensors (e.g. accelerometers, force/torque sensors) and we denote with $\mathbf{y} \in \mathbb{R}^{N_S}$ the vector containing all the measurements. The dynamic variables and the values measured by the sensors can be related by the following set of equations:

$$\mathbf{Y}(\mathbf{q}, \dot{\mathbf{q}})\mathbf{d} + \mathbf{b}_Y(\mathbf{q}, \dot{\mathbf{q}}) = \mathbf{y}, \quad (3)$$

⁴We consider here the fixed base system configuration.

⁵It is worth to notice that here we prefer to adopt the Newton-Euler formalism as an equivalent representation of the system dynamics. More details about this choice in Section 3.3 of [12].

where $\mathbf{Y} \in \mathbb{R}^{Ns \times d}$ and $\mathbf{b}_Y \in \mathbb{R}^{Ns}$. By stacking together (2) and (3) we obtain a linear system of equations in the variable d :

$$\begin{bmatrix} \mathbf{Y}(\mathbf{q}, \dot{\mathbf{q}}) \\ \mathbf{D}(\mathbf{q}, \dot{\mathbf{q}}) \end{bmatrix} \mathbf{d} + \begin{bmatrix} \mathbf{b}_Y(\mathbf{q}, \dot{\mathbf{q}}) \\ \mathbf{b}_D(\mathbf{q}, \dot{\mathbf{q}}) \end{bmatrix} = \begin{bmatrix} \mathbf{y} \\ \mathbf{0} \end{bmatrix}. \quad (4)$$

Equation (4) describes, in general, an overdetermined linear system of equations. The bottom part, corresponding to (2) represents the Newton-Euler equations, while the upper part contains the information coming from the, possibly noisy or redundant, sensors. It is possible to compute the whole-body dynamics estimation by solving the system in (4) for d . One possible approach is to solve (4) in the least-square sense, by using a Moore-Penrose pseudoinverse or a weighted pseudo-inverse.

In the following we perform a different choice. We frame the estimation of d given the knowledge of y and prior information about the model and the sensors in a Gaussian domain by means of a *Maximum-a-Posteriori* (MAP) estimator⁶ such that

$$\mathbf{d}_{MAP} = \arg \max_{\mathbf{d}} p(\mathbf{d}|\mathbf{y}).$$

Since in this framework probability distributions are associated to both the measurements and the model, it suffices to compute the expected value and the covariance matrix of d given y , i.e.

$$\Sigma_{d|y} = (\bar{\Sigma}_D^{-1} + \mathbf{Y}^\top \Sigma_y^{-1} \mathbf{Y})^{-1}, \quad (5a)$$

$$\mu_{d|y} = \Sigma_{d|y} [\mathbf{Y}^\top \Sigma_y^{-1} (\mathbf{y} - \mathbf{b}_Y) + \bar{\Sigma}_D^{-1} \bar{\mu}_D], \quad (5b)$$

where $\bar{\mu}_D$ and $\bar{\Sigma}_D$ are the mean and covariance of the probability distribution $p(d) \sim \mathcal{N}(\bar{\mu}_D, \bar{\Sigma}_D)$ of the model, respectively; Σ_y is the covariance matrix of the distribution $p(y) \sim \mathcal{N}(\mu_y, \Sigma_y)$ related to the measurements. In the Gaussian framework, (5b) corresponds to the estimation of d_{MAP} . It is worth noting that the vector d contains, among the other dynamic variables, an estimate of the joint torque τ for retrieving the inverse dynamics estimation.

5 Experimental Design

Data were collected at Istituto Italiano di Tecnologia (IIT), Genoa, Italy. The experimental set-up encompasses the following different sensor modules: *j*) a wearable suit for the motion tracking, *jj*) two standard force platforms to acquire the ground reaction wrenches, *jjj*) the force/torque sensors of the robot arms.

5.1 Human configuration

Ten healthy adult subjects (7 female, 3 male) have been recruited in the experimental session, height ($166,6 \pm 4,5$ cm) and mass ($61,14 \pm 5,76$ kg). Each subject was

⁶The benefits of the MAP estimator choice are explained in Section 4 of [12].

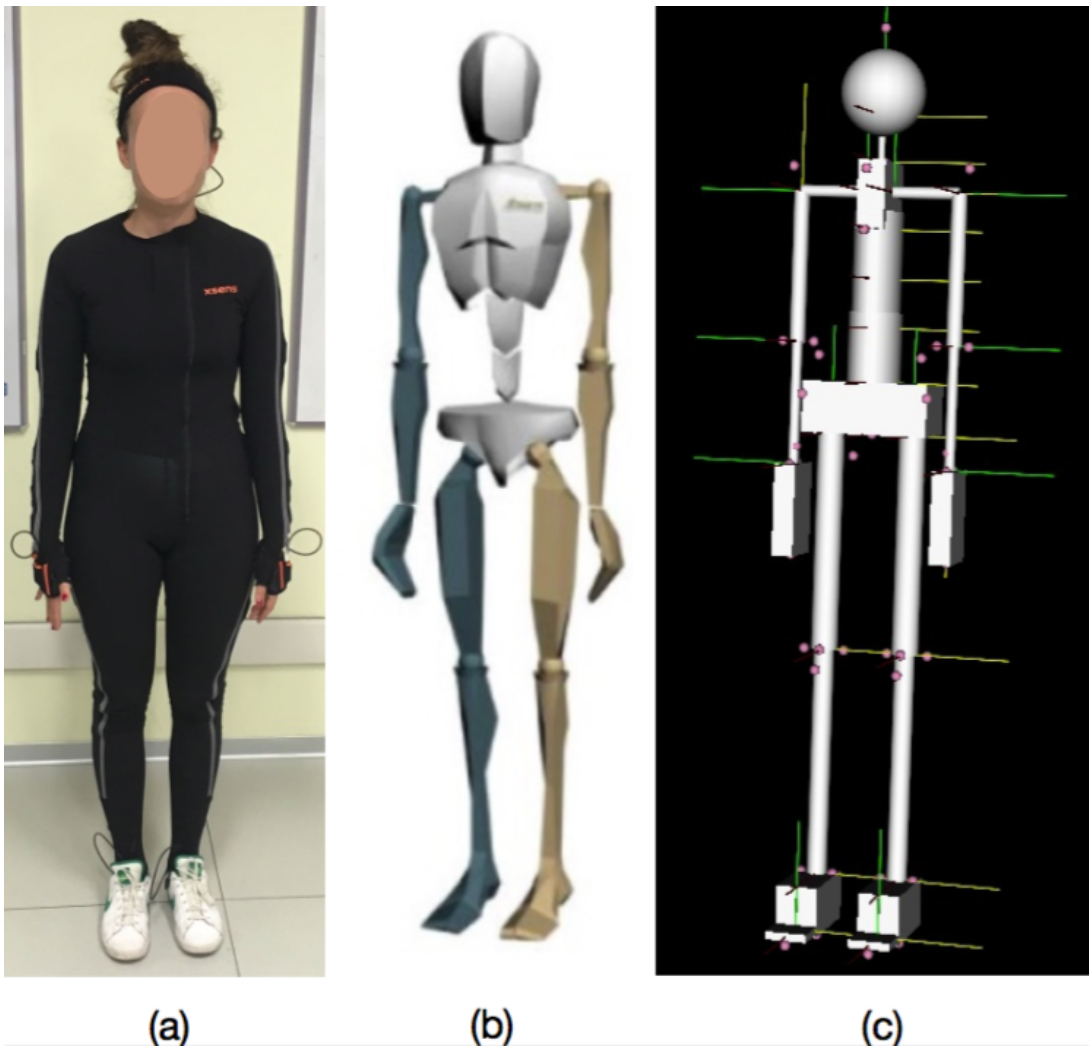


Figure 3: (a) Subject with the motion capture suit. (b) The Xsens MVN model. (c) Model reconstructed in OpenSim by using virtual markers from Xsens acquisition.

provided of a written informative consent before starting the experiment. Kinematics data were acquired by using a full-body wearable lycra suit provided by Xsens Technologies. The wearable suit is composed of 17 wired trackers, (i.e., inertial sensor units-IMUs including an accelerometer, a gyroscope and a magnetometer). The suit has signal transmitters that send measurements to the acquisition unit through a wireless receiver which collects data at a frequency of 240 Hz. The human subject performed the required task standing with the feet on two standard force platforms AMTI OR6 mounted on the ground, while interacting with the robot. Each platform acquired a wrench sample at a frequency of 1 kHz by using AMTI acquisition units.

5.2 Robot configuration

Experiments were conducted on the iCub [16], a full-body humanoid robot (Fig. 4a) with 53-DoFs: 6 in the head, 16 in each arm, 3 in the torso and 6 in each leg. The iCub

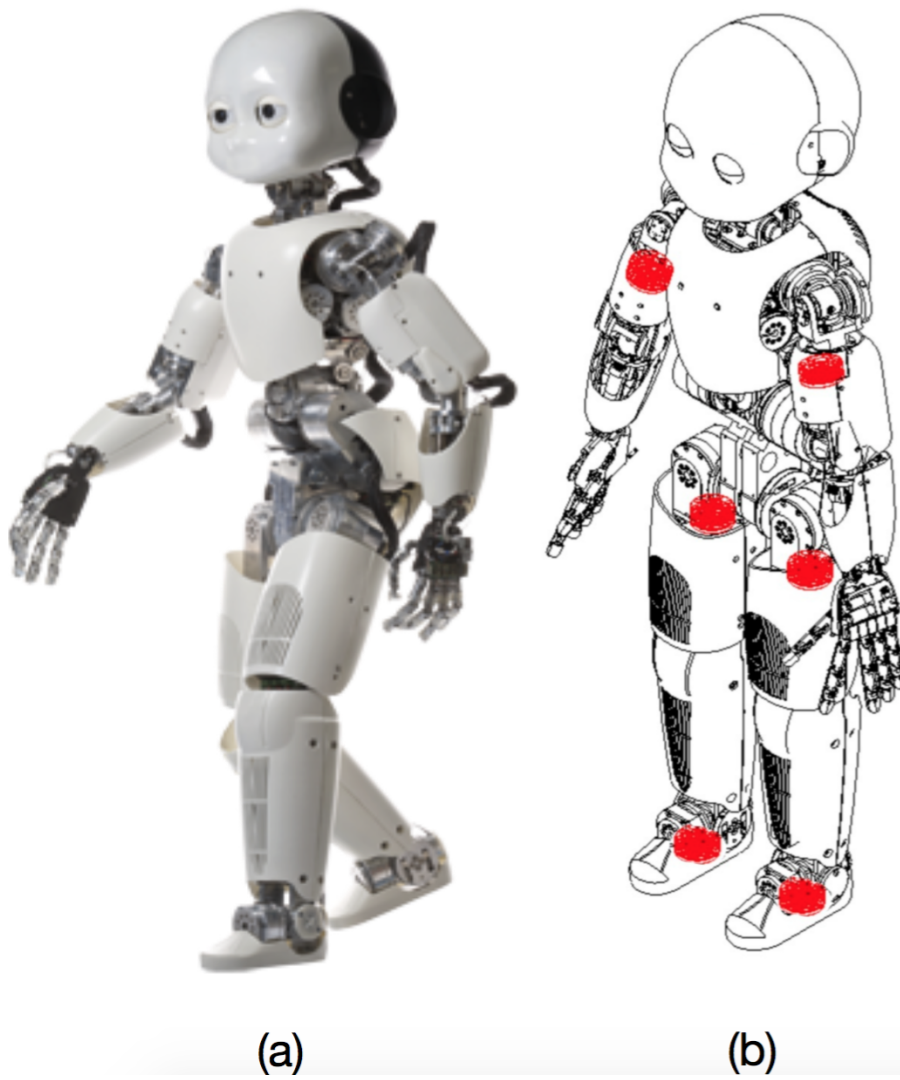


Figure 4: (a) The humanoid iCub. (b) Model of the iCub with the force/torque sensors embedded in the limbs structure.

is endowed with whole-body distributed force/torque sensors, accelerometers, gyroscopes and tactile sensors. Specifically, the limbs are equipped with six force/torque sensors placed in the upper arms, in the upper legs and in the ankles (Fig. 4b). Internal joint torques and external wrenches are estimated through an online whole-body estimation algorithm [18]. Measurements for the wrenches exchanged between the robot and the human are obtained thanks to it. Robot data were collected at a frequency of 100 Hz.

5.3 Procedure protocol

Each subject was asked to wear the suit (Fig. 3a) and to stand on the two force plates by positioning each foot per platform. The robot was located in front of the subject facing him at a known distance from the human foot location (as shown in Fig. 5a).

The mutual feet position was fixed for all the trials (Fig. 5b). The interaction implied that the human grasped and pushed down both robot arms (Fig. 5a) for those tasks that required the interaction. The subject performed:

- a bowing task (*BT*) without (Fig. 6a) and with (Fig. 6b) the robot interaction;
- a squat task (*ST*) without (Fig. 6c) and with (Fig. 6d) the robot.

All subjects had to perform five repetitions of the block composed of the above-mentioned tasks. In each block the order of tasks execution was randomized in order to make each trial as independent as possible among the blocks.

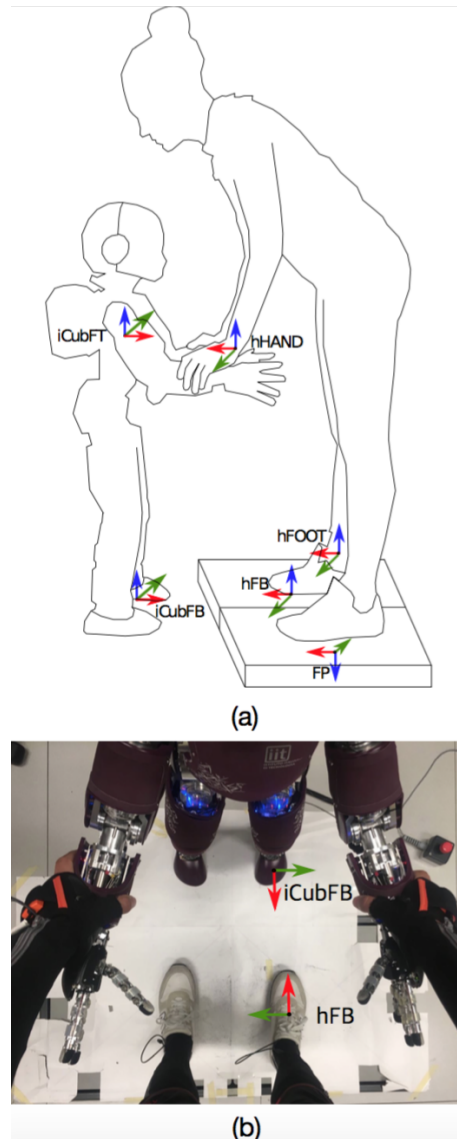


Figure 5: (a) Subject grasps and pushes down the robot arms. The figure shows the reference frames for the force/torque sensor of the robot (iCubFT), the robot fixed base (iCubFB), the force plate (FP), the human fixed base (hFB), the human foot and hand (hFOOT, hHAND) respectively. (b) Top view for the fixed feet position layout.

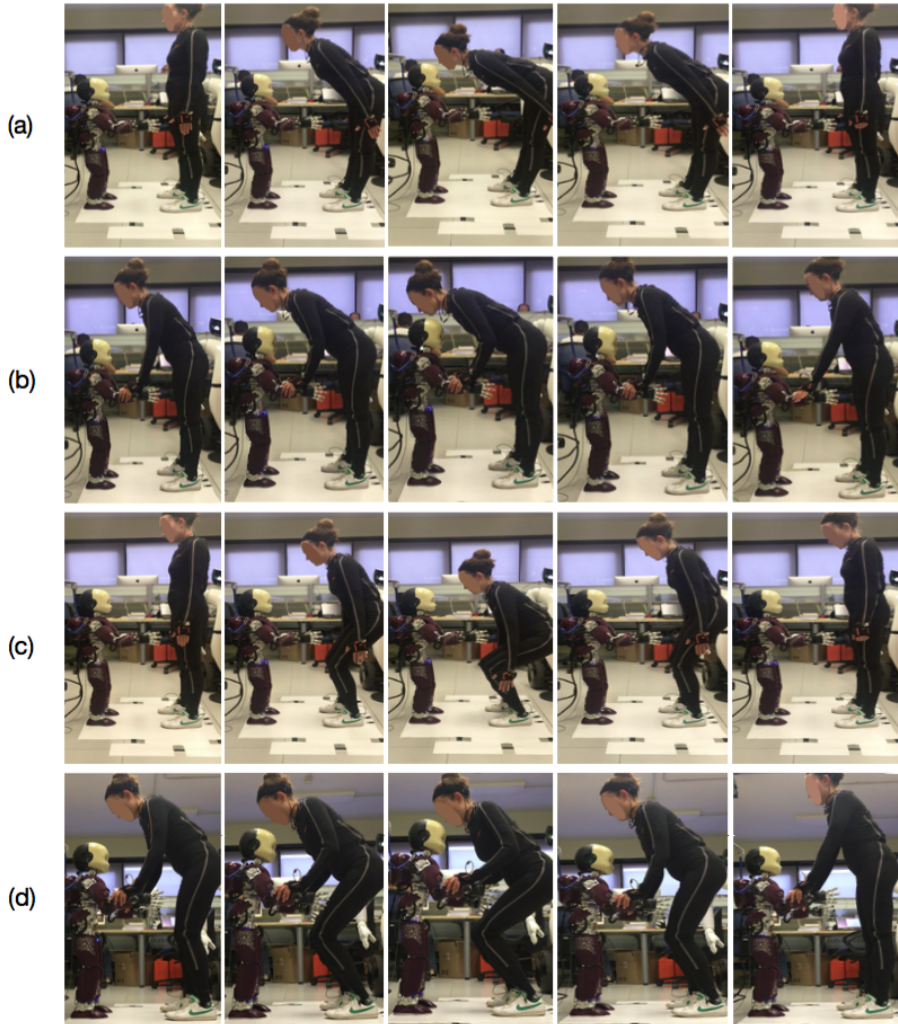


Figure 6: Subject performing: a *BT* without (a) and with (b) the iCub, a *ST* without (c) and with (d) the iCub.

5.4 Data processing

Since the acquisition sampling rate was different among the sources, data are linearly interpolated in order to guarantee the synchronization. An overview of the framework is summarised in Fig. 7. Data coming from the force plates and from the robot (f^x) are considered as acquired from a particular class of net external wrench sensors. Linear acceleration a and angular velocity ω for each link are acquired by Xsens inertial sensors. Xsens data are used as input for the OpenSim [2] IK (Inverse Kinematics) toolbox that allowed to retrieve the joint angles q by matching the marker positions of the OpenSim model (Fig. 3c) and the virtual ones coming from Xsens data. Joint velocities \dot{q} and accelerations \ddot{q} are computed by using a weighted sum of windows of elements, with a third-order polynomial Savitzky-Golay filtering. Also joint accelerations are considered as acquired from a class of DoF acceleration sensors. In general, by considering as inputs data acquired from all above-mentioned sensors and the state

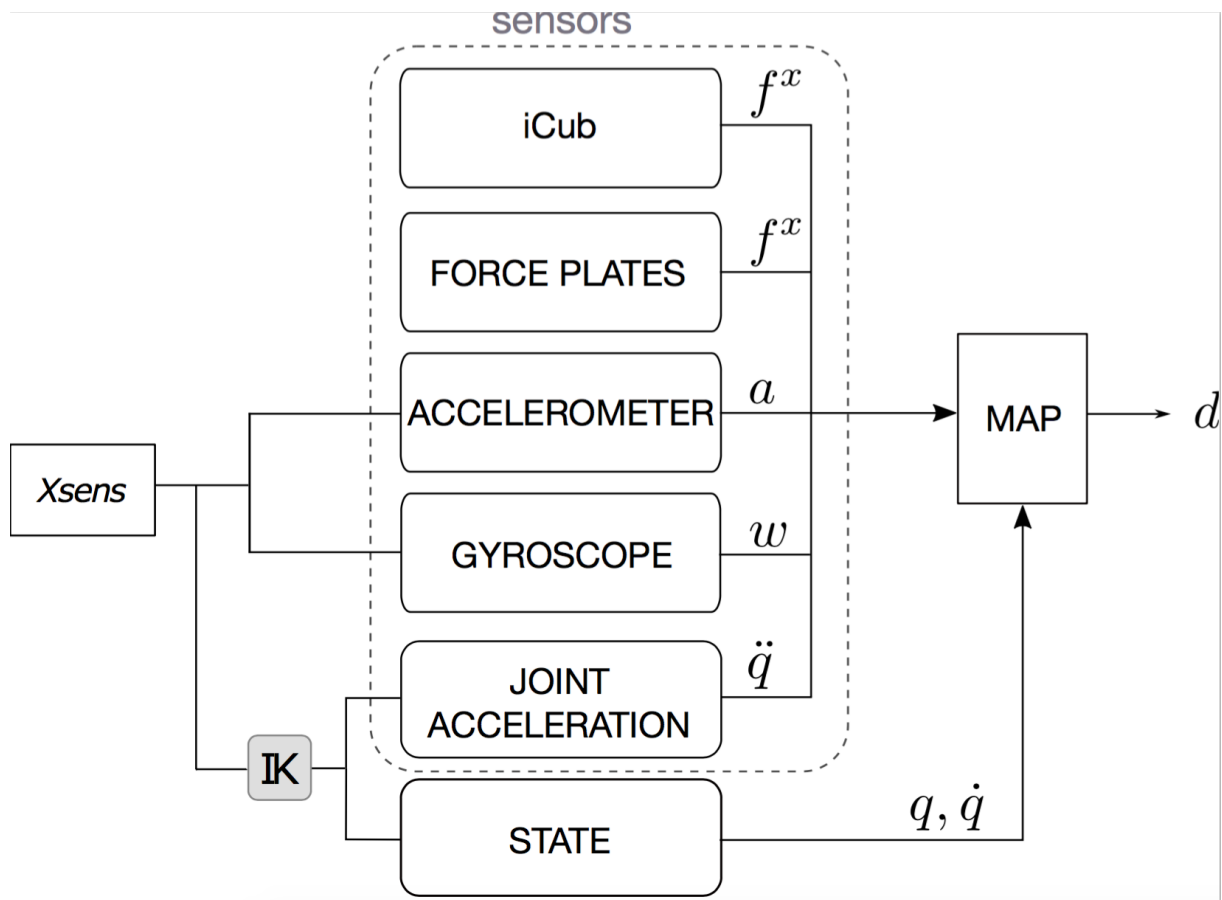


Figure 7: Overview of the MAP estimation algorithm.

(q, \dot{q}) , the MAP estimator provides the estimation of d given y .

6 Experimental Results

In this Section we discuss the evaluation procedure to prove the computation effectiveness of our estimation algorithm. The analysis was mainly performed on Matlab.

6.1 Torques estimation

The core of the experiment consists in estimating the variable d . Among the variables contained in d , the quantities of major interest in our analysis are the torques τ . We consider the internal torques developed along the y axis in which the most significant angle variation is observed. In particular, we take into account the torque at the hip for BT and the knee for ST . Since the torque estimation provides qualitatively a comparable result for both the two sides of the human body, it is exhaustive to show only the torques associated to one side, e.g. the right one. The value of the torque mostly depends on the kinematics and further on the inertial parameters of the subject and

therefore, in order to compare torques across different subjects, it has to be normalized by considering the maximum and minimum values of each subject's torque. Figures ??-?? show the mean and the standard deviation of the right hip τ estimation without and with the interaction with the robot, respectively. Figures ??-?? show the same quantities for the torques at the right knee in a *ST* task.

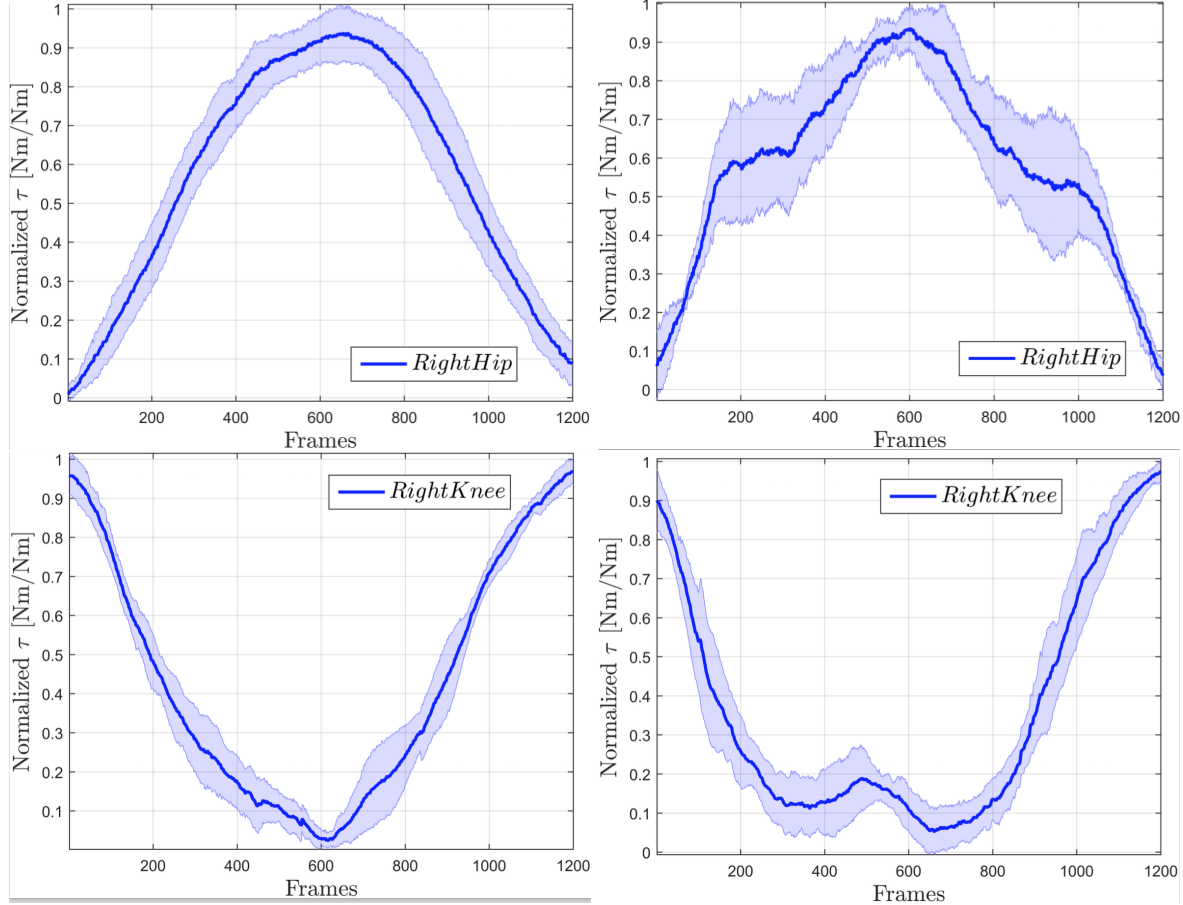


Figure 8: *Inter-subjects analysis*: normalized torques of 10 subjects (mean and standard deviation) for right hip in *BT* without (a) and with (b) robot, for right knee in *ST* without (c) and with (d) robot.

6.2 Robustness test

To test the robustness of the method with respect to modeling errors we asked one subject to perform the *BT* with the robot in two different configurations, i.e. *with* and *without* an additional mass (W) of 6 kg roughly positioned in correspondence of the torso center of mass. The MAP computation was performed by considering as algorithm inputs the following cases (see Table 1):

- *case A*: model of the subject without W and measurements acquired while performing the *BT* with W ;

- *case B*: model of the subject without W and measurements acquired while performing the BT without W .

Since in both the cases the analysis is performed with the model of the subject without W , in order to highlight a lower reliability for the model used in *case A* computation, it is assigned a value to the model variance ⁷ equal to 10^{-1} (different from the value of variance equal to 10^{-4} assigned for the *case B*).

Table 1: Cases for the MAP evaluation.

| | case A | case B |
|------------------------------|------------------------|----------------|
| model | without W | without W |
| measurements | with W | without W |
| Σ model | 10^{-1} | 10^{-4} |
| MAP torque estimation | $\tau_{(model+6\ kg)}$ | τ_{model} |

By exploiting the linearity property of the system we started by considering the following expression for the torques

$$\tau_{(model+6\ kg)} - \tau_{model} = \tau_{6\ kg} \quad (6)$$

where $\tau_{6\ kg}$ is the theoretical torque due to the additional W positioned on the torso⁸. Given (6), it is possible to retrieve the error ε_τ on the τ estimation for the subject with W , due to *case A*:

$$\varepsilon_\tau = |\tau_{(model+6\ kg)} - \tau_{model}| - \tau_{6\ kg} \quad (7)$$

We computed (7) by using the OpenSim ID (Inverse Dynamics) toolbox as well, in order to evaluate its effectiveness with respect to the modeling errors. Figures ??-?? provide the mean and the standard deviation of the torque estimation by means of the MAP algorithm and the OpenSim software, respectively. Figure ?? shows the comparison between the computation of the error in (7) for both the above methods: the error is higher in OpenSim computation than in MAP since OpenSim does not offer the possibility of setting the model reliability in the computation.

6.3 Incremental sensor fusion analysis

Since a distinctive feature of our framework consists in the possibility of building (3) for different sources of measurement, we here investigate the advantage in using this algorithm for the dynamics estimation. We consider three sets of y equations for:

1. the two force plates:

$$y_{FP} = {}^{FP}X_{hFOOT} f_{hFOOT} \quad (8)$$

⁷We refer here to the model covariance associated to the model as a diagonal matrix where each element of the diagonal is the variance value.

⁸We consider a simple 2-DoF system (see [12]) in which the position of W and the hip joint angle are known.

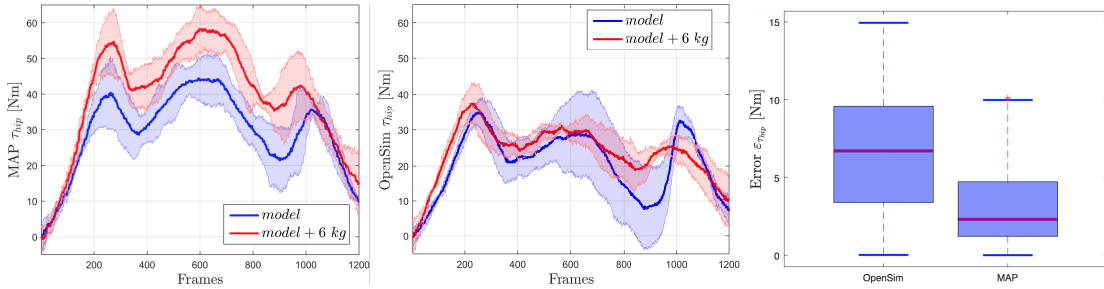


Figure 9: *Intra-subjects analysis*: mean and standard deviation of τ (i.e., the sum of the τ estimated at the hips) among five repetitions of the *BT* performed by a subject computed for *case A* (red) and *case B* (blue) by means of (a) MAP algorithm and (b) by using the OpenSim ID (Inverse Dynamics) toolbox. (c) Box plots of the torque estimation error ε_τ computed in (7) with MAP (on the right) and with OpenSim (on the left). It shows that MAP is a method more robust to the modelling errors since it gives the possibility of weighting the reliability of the model by properly setting the related covariance matrix.

where it is used the trasformation matrix⁹ \mathbf{X} between the human foot reference frame (*hFOOT*) and each force plate frame (*FP*);

2. the IMUs embedded in the suit:

$$\mathbf{y}_{IMU} = {}^{IMU}\mathbf{X}_L \mathbf{a}_L \quad (9)$$

by exploiting the trasformation between each human link frame L on which the IMU is attached and that particular IMU reference frame (Fig. 2a);

3. the force/torque sensors of the two arms of the robot:

$$\mathbf{y}_{iCubFT} = {}^{iCubFT}\mathbf{X}_{hHAND} \mathbf{f}_{hHAND} \quad (10)$$

for which it is necessary knowing the transformation between each human hand frame (*hHAND*) to the robot sensor frame (*iCubFT*).

A general overview of the above-mentioned frames is shown in Fig. 5a. We want to prove that, by adding progressively the different sensors data at each MAP computation, the variance associated to the estimated dynamic variables consequently decreases, making the estimation more reliable. In particular, we build (3) for three different cases (Fig. 10a) :

case 1) $y = [\ddot{\mathbf{q}}, \mathbf{y}_{FP}]$

case 2) $y = [\ddot{\mathbf{q}}, \mathbf{y}_{FP}, \mathbf{y}_{IMUs}]$

case 3) $y = [\ddot{\mathbf{q}}, \mathbf{y}_{FP}, \mathbf{y}_{IMUs}, \mathbf{y}_{iCubFT}]$.

⁹See [6] for the definition of the trasformation matrix between two reference frames.

The MAP computation is performed for each case since the incremental addition of a sensor includes each time a new information on the analysis. For this analysis we take into account a task involving the robot (*BT*) in order to include the robot sensor measurements in the computation. Among the variables in \mathbf{d} we consider again the torque τ (i.e., right and left ankle and hip) and the variance along the axis of major relevance y .

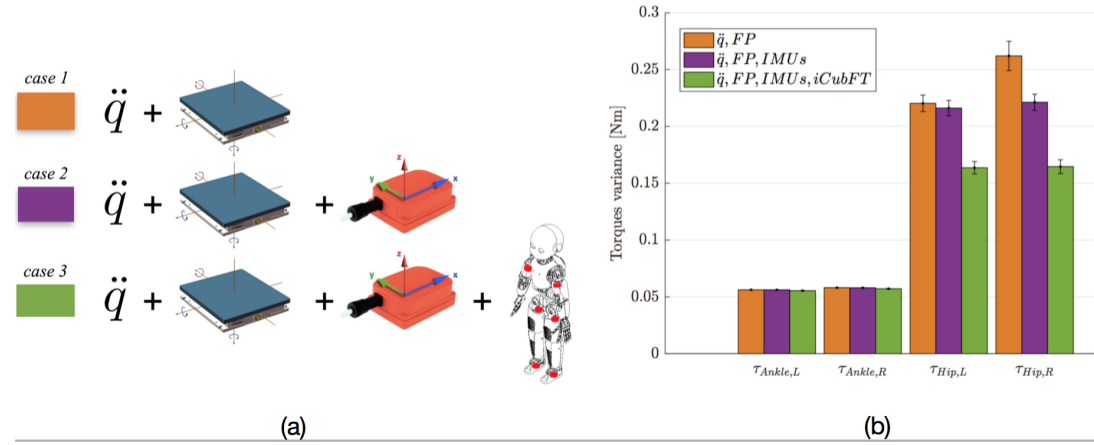


Figure 10: (a) Description of three cases for progressive addition of sensors. (b) *Inter-subjects analysis*: mean variance of τ at the left and right ankle and hip among five repetitions of the *BT* performed by ten subjects computed by MAP with the three different version of the measurements vector y .

Passing progressively from *case 1* to *case 3* (Fig. 10a) the variance associated to the torques decreases¹⁰. In Fig. 10b we show the decreasing behaviour of the mean variance of the torque at the hips and at the ankles computed between ten subjects. The variance values on the ankles do not change significantly among the three different configurations of sensors since the ankle torque estimation depends mostly on the contribution of the force plates that are included in all the three cases of the computation. Conversely, a significant decreasing behaviour is present in the values associated to the hips. In this case the contribution of the three sources of sensors becomes important since the torque estimation at the hips are affected by the all sensors.

7 Conclusions and Future Works

One of the aim of the presented framework is the estimation of dynamic variables of a human being while is physically interacting with a robot. This paper is the extended version of the probabilistic framework explored in [12] but we introduced here a more complex model (23 vs 3 links and 22 vs 2 joints) and we found that our framework is able

¹⁰In order to assess the statistical significance of results, a paired-samples *t-test* is performed firstly between *case 1* and *case 2* (2 sensors vs 3 sensors) and then between *case 2* and *case 3* (3 sensors vs all sensors). Torque variances statistically significant, *p-value* < 0.05.

to estimate human dynamics variables even in presence of a multi-DoFs model. We performed also a comparison with the well-established biomechanical software OpenSim: the results were promising depicting a good bent of our framework in modelling possible inaccuracies in the model.

In this paper the endeavour was to retrieve an estimation of the human dynamics by means of the MAP algorithm and to this purpose the robot was considered as a *passive* forces measurer. But since the human dynamics is of pivotal importance for a control design aimed at considering the *human in the loop*, the forthcoming idea will be to provide in real-time the robot with the human force feedback that could be used either as a tool for *reactive* human-robot collaboration (implying a robot reactive control) and, in a long-term perspective, for *predictive* collaboration, for enhancing remarkably the interaction naturalness. Thus, in the near future a new robot controller has to be designed in order that the robot can adapt and adjust the interaction strategy accordingly.

In this work we applied the proposed approach to human models composed of 1-DoF revolute joints, by using the classical formalism widespread in robotics [6]. In particular we combined this type of joints to obtain a series of joints with a high number of DoFs, that however are only a rough approximation of the complexity exhibited by real-life biomechanical joints. While we chose this joint model for an initial exploration of the method, the proposed algorithm is not limited to this particular choice. In particular the properties of any joint (with an arbitrary number of DoFs) can be encapsulated in an interface where the relative position, velocity and acceleration of the two bodies connected by it are described by arbitrary functions of joint coordinates variables and their derivatives that can then be directly inserted in (2) and (3). In this way, any kind of joint modelling can be described under this formalism (e.g., complex non-linear models, models of biomechanical joints based on tabulated data obtained from human experiments [3]). A possible implementation is presented in [20], where it is used in the context of biomechanical simulations. In the future we plan to translate this type of results in our framework, to generalize our method to arbitrarily complex musculoskeletal models.

References

- [1] H. B. Amor, G. Neumann, S. Kamthe, O. Kroemer, and J. Peters. Interaction primitives for human-robot cooperation tasks. In *2014 IEEE International Conference on Robotics and Automation (ICRA)*, pages 2831–2837, May 2014.
- [2] S. L. Delp, F. C. Anderson, A. S. Arnold, P. Loan, A. Habib, C. T. John, E. Guendelman, and D. G. Thelen. Opensim: Open-source software to create and analyze dynamic simulations of movement. *IEEE Transactions on Biomedical Engineering*, Nov 2007.
- [3] S. L. Delp, J. P. Loan, M. G. Hoy, F. E. Zajac, E. L. Topp, and J. M. Rosen. An interactive graphics-based model of the lower extremity to study orthopaedic sur-

- gical procedures. *IEEE Transactions on Biomedical engineering*, 37(8):757–767, 1990.
- [4] J. Denavit and R. S. Hartenberg. A kinematic notation for lower-pair mechanisms based on matrices. *Trans. of the ASME. Journal of Applied Mechanics*, 22:215–221, 1955.
 - [5] R. Drillis, R. Contini, and M. Bluestein. Body segment parameters; a survey of measurement techniques. *Artificial limbs*, 25, 1964.
 - [6] R. Featherstone. *Rigid Body Dynamics Algorithms*. Springer-Verlag New York, Inc., Secaucus, NJ, USA, 2007.
 - [7] T. Flash and N. Hogan. The coordination of arm movements: an experimentally confirmed mathematical model. *Journal of Neuroscience*, 5(7):1688–1703, 1985.
 - [8] G. Guerra-Filho and A. Biswas. The human motion database: A cognitive and parametric sampling of human motion. In *Face and Gesture 2011*, pages 103–110, March 2011.
 - [9] E. P. Hanavan. A mathematical model of human body. Technical report, Air force aerospace medical research lab Wright-Patterson AFB OH, 1964.
 - [10] I. P. Herman. *Physics of the human body*, chapter Terminology, the standard human, and scaling. Springer, 2007.
 - [11] H. Kuehne, H. Jhuang, E. Garrote, T. Poggio, and T. Serre. Hmdb: A large video database for human motion recognition. In *2011 International Conference on Computer Vision*, pages 2556–2563, Nov 2011.
 - [12] C. Latella, N. Kuppuswamy, F. Romano, S. Traversaro, and F. Nori. Whole-body human inverse dynamics with distributed micro-accelerometers, gyros and force sensing. *Sensors*, 16(5):727, 2016.
 - [13] Y. Maeda, T. Hara, and T. Arai. Human-robot cooperative manipulation with motion estimation. In *Intelligent Robots and Systems, 2001. Proceedings. 2001 IEEE/RSJ International Conference on*, volume 4, pages 2240–2245, 2001.
 - [14] C. Mandery, Ö. Terlemez, M. Do, N. Vahrenkamp, and T. Asfour. Unifying representations and large-scale whole-body motion databases for studying human motion. *IEEE Transactions on Robotics*, 32(4):796–809, Aug 2016.
 - [15] J. E. Marsden and T. S. Ratiu. *Introduction to Mechanics and Symmetry: A Basic Exposition of Classical Mechanical Systems*. Springer Publishing Company, Incorporated, 2010.
 - [16] G. Metta, L. Natale, F. Nori, G. Sandini, D. Vernon, L. Fadiga, C. von Hofsten, K. Rosander, M. Lopes, J. Santos-Victor, A. Bernardino, and L. Montesano. The

icub humanoid robot: An open-systems platform for research in cognitive development. *Neural Networks*, 23(8–9):1125 – 1134, 2010. Social Cognition: From Babies to Robots.

- [17] S. Miossec and A. Kheddar. Human motion in cooperative tasks: Moving object case study. In *Robotics and Biomimetics, 2008. ROBIO 2008. IEEE International Conference on*, pages 1509–1514, Feb 2009.
- [18] F. Nori, S. Traversaro, J. Eljaik, F. Romano, A. Del Prete, and D. Pucci. icub whole-body control through force regulation on rigid non-coplanar contacts. *Frontiers in Robotics and AI*, 2015.
- [19] D. Roetenberg, H. Luinge, and P. Slycke. Xsens mvn: full 6dof human motion tracking using miniature inertial sensors. Technical report, Xsens Motion Technologies BV, 2009.
- [20] A. Seth, M. Sherman, P. Eastman, and S. Delp. Minimal formulation of joint motion for biomechanisms. *Nonlinear dynamics*, 62(1-2):291–303, 2010.
- [21] Ö. Terlemez, S. Ulbrich, C. Mandery, M. Do, N. Vahrenkamp, and T. Asfour. Master motor map (mmm) - framework and toolkit for capturing, representing, and reproducing human motion on humanoid robots. In *2014 IEEE-RAS International Conference on Humanoid Robots*, pages 894–901, Nov 2014.
- [22] D. A. Winter. *Biomechanics and motor control of human movement*, chapter Anthropometry. Wiley, 1990.
- [23] J. Wojtusch and O. von Stryk. Humod - a versatile and open database for the investigation, modeling and simulation of human motion dynamics on actuation level. In *2015 IEEE-RAS 15th International Conference on Humanoid Robots (Humanoids)*, pages 74–79, Nov 2015.
- [24] M. Yeadon. The simulation of aerial movement ii. a mathematical inertia model of the human body. *Journal of Biomechanics*, 23(1):67–74, 1990.